Parasitol Res (2010) 107:337–353
DOI 10.1007/s00436-010-1866-2

ORIGINAL PAPER

Enhancement of the drug susceptibility of a triclabendazole-resistant isolate of *Fasciola hepatica* using the metabolic inhibitor ketoconazole

Catherine Devine · Gerard P. Brennan · Carlos E. Lanusse · Luis I. Alvarez · Alan Trudgett · Elizabeth Hoey · Ian Fairweather

Received: 23 February 2010 / Accepted: 29 March 2010 / Published online: 30 May 2010

Abstract A study has been carried out to investigate whether the action of triclabendazole (TCBZ) is altered by using the metabolic inhibitor, ketoconazole (KTZ) to inhibit the cytochrome P450 (CYP 450) system within *Fasciola hepatica*. The Oberon TCBZ-resistant and Cullompton TCBZ-susceptible isolates were used for these experiments. The CYP 450 enzyme system was inhibited by a 2 h pre-incubation in KTZ (40 μM). Flukes were then incubated for a further 22 h in NCTC medium containing either KTZ; KTZ + nicotinamide adenine dinucleotide phosphate (NADPH; 1 nM); KTZ + NADPH + TCBZ (15 μg/ml); or KTZ + NADPH + triclabendazole sulphoxide (TCBZ.SO;15 μg/ml). Morphological changes resulting from drug treatment and following metabolic inhibition were assessed using scanning electron microscopy. After treatment with either TCBZ or TCBZ.SO alone, there was greater disruption to the TCBZ-susceptible isolate than the TCBZ-resistant isolate. However, co-incubation with KTZ and TCBZ/TCBZ.SO led to more severe surface changes to the TCBZ-resistant isolate than with each drug on its own, with greater swelling and blebbing of the tegument and even the loss of the apical plasma membrane in places. With the Cullompton isolate, there was limited potentiation of drug action in combination with KTZ, and only with TCBZ.SO. The results support the concept of altered drug metabolism within TCBZ-resistant isolates and indicate that this process may play a role in the development of drug resistance.

C. Devine · G. P. Brennan · A. Trudgett · E. Hoey · I. Fairweather (✉)
Parasite Therapeutics Group, School of Biological Sciences, Medical Biology Centre, The Queen's University of Belfast, 97 Lisburn Road, Belfast BT9 7BL Northern Ireland, UK
e-mail: i.fairweather@qub.ac.uk

C. E. Lanusse · L. I. Alvarez
Laboratorio de Farmacología, Departamento de Fisiopatología, Facultad de Ciencias Veterinarias, Universidad Nacional del Centro de la Provincia de Buenos Aires, Campus Universitario (UNCPBA), 7000 Tandil, Argentina

Introduction

Anthelmintic drugs currently are the main method used to control parasitic infections, but the development of drug-resistant populations threatens management strategies. *Fasciola hepatica* is one of the most important parasites that affect animal health in the UK and throughout Europe, and the emergence of populations resistant to triclabendazole (TCBZ), the current drug of choice, is a worrying prospect, as no new *Fasciola*-specific drugs are in development. New avenues need to be investigated in order to optimise drug use and maintain productivity. Within the host, xenobiotic compounds are metabolised by biotransformation enzyme systems, such as the flavin monooxygenase (FMO) and cytochrome P-450 (CYP 450) systems, into more polar metabolites which are easier to excrete (Cvilink et al. 2009).

Parasites, such as *F. hepatica*, have been shown to have the ability to metabolise anthelmintic compounds (Solana et al. 2001, 2009; Mottier et al. 2004; Robinson et al. 2004; Alvarez et al. 2005). Within different isolates of *F. hepatica*, studies have shown marked differences in the ability to metabolise TCBZ and this has been suggested as a possible mechanism of resistance within TCBZ-resistant isolates. The metabolism of triclabendazole (TCBZ) to

triclabendazole sulphoxide (TCBZ.SO) and TCBZ.SO to triclabendazole sulphone ($TCBZ.SO_2$) has been shown to be significantly higher in TCBZ-resistant isolates of *F. hepatica* (Robinson et al. 2004; Alvarez et al. 2005). This has been linked to a possible increase in the expression of the metabolic enzymes. This increased metabolism of TCBZ to less active metabolites provides the resistant flukes with an effective mechanism to evade the action of TCBZ (Brennan et al. 2007), as it is generally accepted that the sequential oxidation of benzimidazole anthelmintics leads to more polar and less active metabolites (Prichard et al. 1985).

Oxidation, reduction or hydrolysis represent the phase I of the metabolism of drugs and the most important enzymes involved in phase I biotransformation are CYP 450 enzymes (Cvilink et al. 2009). CYP 450's commonly catalyse mono-oxygenation of substrates (Cvilink et al. 2009). The existence of CYP 450 enzyme systems has been shown in a number of helminth parasites: the trematodes *Dicrocoelium dendriticum*, *F. hepatica* and *Schistosoma mansoni*; the cestode, *Moniezia expansa*; and a number of nematodes, including *Haemonchus contortus* and *Caenorhabditis elegans* (Kerboeuf et al. 1995; Kotze 1997, 1999, 2000; Gotoh 1998; Alvinerie et al. 2001; Solana et al. 2001, 2009; Saeed et al. 2002; Kotze et al. 2006; Cvilink et al. 2008, 2009). A CYP 450-mediated pathway has been implicated in the metabolism of TCBZ in *F. hepatica* and probably plays a greater role in the conversion of TCBZ.SO to $TCBZ.SO_2$, rather than the initial TCBZ to TCBZ.SO conversion (Alvarez et al. 2005).

Inhibitors of FMO and CYP 450 enzymatic systems have been shown to interfere with the biotransformation of benzimidazole anthelmintics both in vitro and in vivo (Lanusse and Prichard 1993; Alvarez et al. 2005; Virkel et al. 2009). The combination of a FMO inhibitor, methimazole with TCBZ lead to more severe morphological changes in a TCBZ-resistant isolate than when incubated in the drug alone (Devine et al. 2009). Similarly, TCBZ co-incubation with piperonyl butoxide (PB), a CYP 450 inhibitor, lead to more severe surface changes in the same TCBZ-resistant isolate than when the flukes were incubated in TCBZ or TCBZ.SO alone (Devine et al. 2010a).

Ketoconazole (KTZ) is a broad-spectrum antifungal agent and a known selective inhibitor of CYP 450 3A-mediated reactions, with concentrations higher than 10 μM possibly inhibiting the metabolic activities of other CYP 450 isoenzymes (Newton et al. 1995; Bourrie et al. 1996; Zhang et al. 2002). This study continues previous morphological (Devine et al. 2009, 2010a, b) and biochemical investigations (Alvarez et al. 2005) on the role of altered drug metabolism in the development of resistance to TCBZ in *F. hepatica*. The

Table 1 Drug and inhibitor combinations

KTZ (40μM)	NADPH (1nM)	TCBZ (15μg/ml)	TCBZ.SO (15μg/ml)
✓			
✓	✓		
✓	✓	✓	
✓	✓		✓
		✓	
			✓

KTZ ketoconazole, *NADPH* nicotinamide adenine dinucleotide phosphate, *TCBZ* triclabendazole, *TCBZ.SO* triclabendazole sulphoxide

Figs. 1–8 Scanning electron micrographs (SEMs) of the tegumental surface of the liver fluke, *Fasciola hepatica* (Cullompton [Figs. 1 and 8] and Oberon [Figs. 2–7] isolates) following 24 h in vitro treatment with KTZ

1 A low-power image of the ventral surface of the apical cone region. *OS* oral sucker, *GP* gonopore; *bar* 200 μm. *Inset* shows a high-power image of a spine (*S*), which appears normal; *bar* 10 μm

2 A low-power image of the dorsal surface of the apical cone region. *OS*, oral sucker; *bar* 200 μm. *Inset* is a high-power image showing the normal appearance of a spine (*S*) and the surrounding tegument; *bar* 10 μm

3 Ventral surface of the anterior midbody region showing slight swelling of the tegument (*arrows*) between the spines (*S*); *bar* 50 μm. *Inset* is a high-power image of a spine (*S*), which retains a normal morphology; *bar* 10 μm

4 Dorsal surface of the anterior midbody region showing swelling of the interspinal tegument (*arrow*) and of the tegument covering (*arrow head*) the spines (*S*); *bar* 50 μm. *Inset* is a high-power image of a spine (*S*) showing the swelling of its tegumental covering (*arrow*); *bar* 10 μm

5 A low-power image of the ventral surface of the posterior midbody region showing swelling (*arrow*) and furrowing (*F*) of the interspinal tegument. *S*, spine; *bar* 50 μm. *Inset* shows a high-power image of a spine (*S*) and the swelling of the tegument (*arrow*) around it; *bar* 10 μm

6 Dorsal surface of the posterior midbody region showing swelling (*arrow*) and furrowing (*F*) of the inter-spinal tegument. The tegument covering the spines is swollen (*arrow head*). *S* spine; *bar* 50 μm. *Inset* is a higher magnification image of a spine (*S*) and the swelling of the tegument covering it (*asterisk*), which has obscured the spinelets. The surface has a roughened appearance (*arrow*); *bar* 10 μm

7 Ventral surface of the tail region showing swelling (*arrows*) and furrowing (*F*) of the interspinal tegument. There are patches of roughened tegument (*arrow head*) over the tail surface; *S* spine; *bar* 50 μm. *Inset* shows a high-power image of a spine (*S*) and the swelling of the tegument surrounding it (*arrow head*). The tegument covering the spines is swollen and has completely enclosed the spinelets (*arrow*); *bar* 10 μm

8 A high-power image of the ventral surface of the tail region showing swelling (*arrow*) and furrowing (*F*) of the interspinal tegument. *S* spine; *bar* 10 μm

aim of this study was to investigate whether the action of TCBZ was altered, in TCBZ-susceptible and -resistant isolates, after CYP 450 inhibitions with KTZ. Changes to the surface morphology of the fluke were assessed using scanning electron microscopy (SEM). Attention focused on the tegument as it is the main site of TCBZ entry (Mottier et al. 2006a; Toner et al. 2009, 2010) and it represents a site of considerable biochemical, physiological, and immune interaction between the host and parasite (Fairweather et al. 1999).

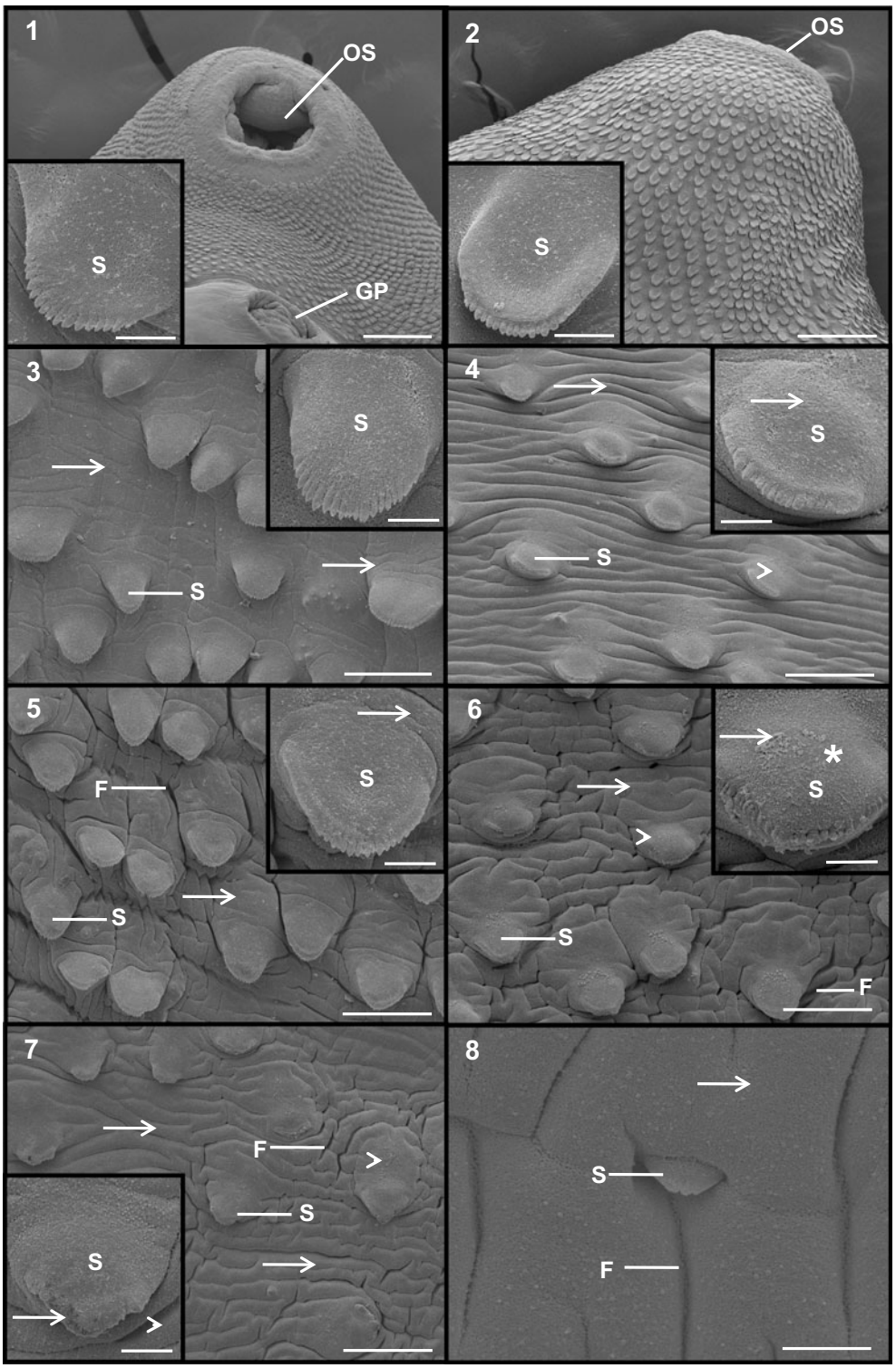

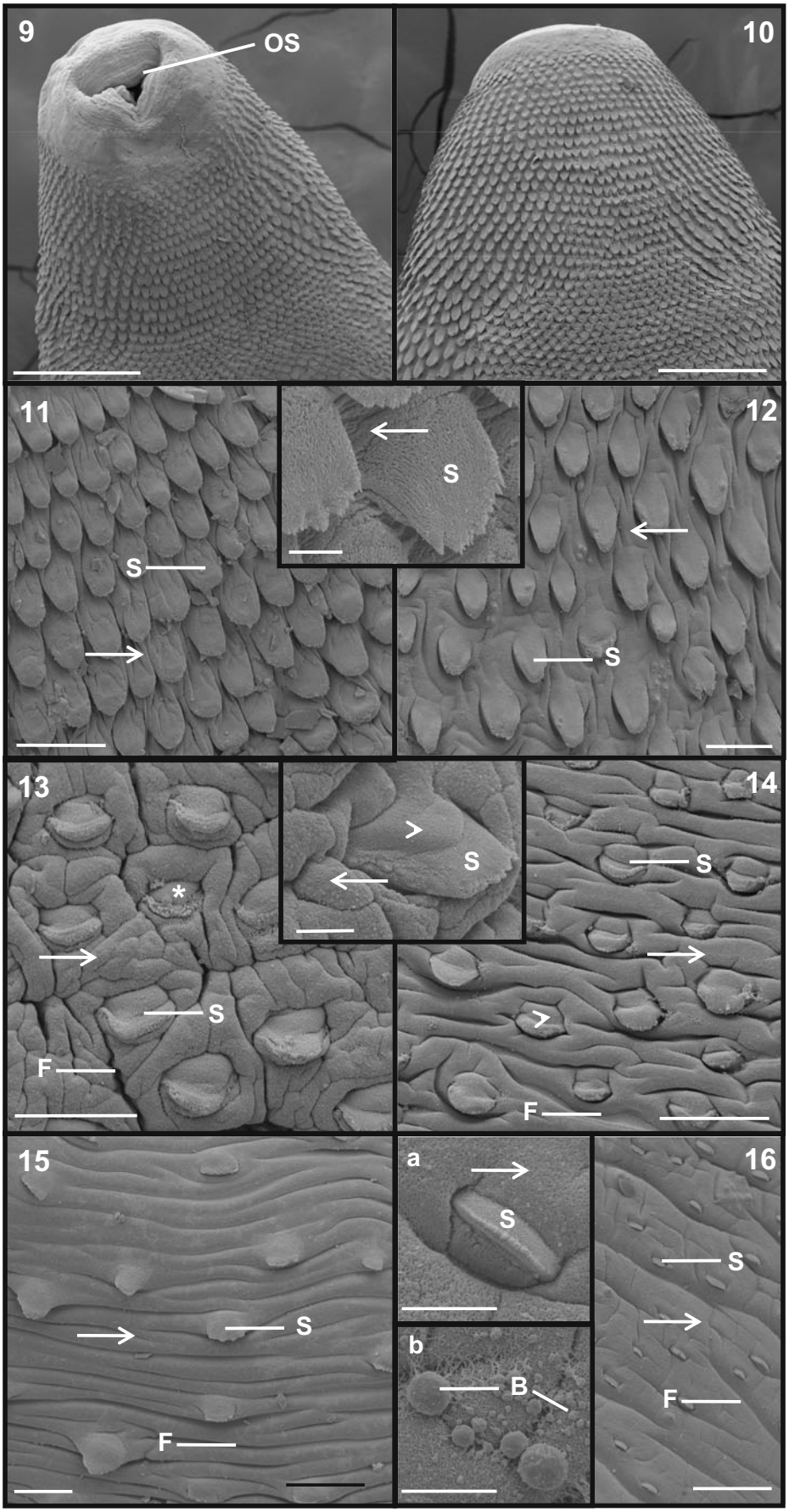
9
OS
10
11
S
S
12
S
13
S
*
S
F
14
S
F
15
S
F
a
S
b
B
16
S
F

Figs. 9–16 Scanning electron micrographs (SEMs) of the tegumental surface of the liver fluke, *F. hepatica* (Cullompton [Figs. 14 and 16] and Oberon [Figs. 9–13 and 15] isolates) following 24 h in vitro treatment with KTZ + NADPH

9 A low-power image of the ventral surface of the oral cone region. *OS* oral sucker; *bar* 400 μm

10 A low-power image of the dorsal surface of the apical cone region; *bar* 300 μm

11 Ventral surface of the apical cone region showing slight swelling of the tegument (*arrow*) between the spines (*S*); *bar* 50 μm. *Inset* shows a high-power image of a spine (*S*) and the slight swelling of the interspinal tegument (*arrow*); *bar* 10 μm

12 A low-power image of the dorsal surface of the apical cone region showing slight swelling of the interspinal tegument (*arrow*). *S* spine; *bar* 50 μm

13 Ventral surface of the midbody region showing swelling (*arrow*) and furrowing (*F*) of the interspinal tegument. The tegument covering the spines is also swollen (*asterisk*); *bar* 50 μm. *Inset* is a high magnification image of a spine (*S*) and the associated swelling of the tegument covering (*arrow head*) and surrounding (*arrow*) it; *bar* 10 μm

14 Midbody region of the dorsal surface showing swelling of the tegument covering (*arrow head*) and between (*arrow*) the spines (*S*). Tegumental furrowing (*F*) was also evident; *bar* 50 μm

15 Ventral surface of the tail region showing swelling (*arrow*) and furrowing (*F*) of the interspinal tegument. *S* spine; *bar* 50 μm

16 A low-power image of the dorsal surface of the tail region showing swelling (*arrow*) and furrowing (*F*) of the tegument between the spines (*S*); *bar* 50 μm. *Inset a* shows a high-power image of a spine (*S*) and the swelling (*arrow*) of the tegument around it; *bar* 10 μm. *Inset b* shows a high magnification image of tegumental blebbing (*B*); *bar* 10 μm

Materials and methods

Adult male Sprague Dawley rats were each infected with 20 metacercarial cysts of either the Oberon TCBZ-resistant or Cullompton TCBZ-susceptible isolate of *F. hepatica*. The Oberon isolate originated on a farm where TCBZ resistance was suspected, in Oberon, New South Wales, Australia in 1999, and has since been maintained in the laboratory. The isolate has been shown to be resistant to TCBZ action as the drug has limited efficacy against Oberon isolates in vivo and in vitro (Walker et al. 2004; Keiser et al. 2007). The Cullompton isolate originated from a field isolate in Cullompton, Devon, England. This isolate has been shown to be susceptible to TCBZ action in vivo and to its sulphoxide metabolite in vitro (Robinson et al. 2002; McCoy et al. 2005; McConville et al. 2006, 2009a, b; Meaney et al. 2006, 2007; Halferty et al. 2008, 2009; Hanna et al. 2010; Devine et al. 2009, 2010a, b; Toner et al. 2009, 2010).

Adult flukes (at least 12 weeks old) were removed from the bile ducts of rats under sterile conditions in a laminar flow cabinet and washed repeatedly in warm (37°C) NCTC 135 culture medium (pH 7.4) containing antibiotics (penicillin 50 IU/ml; streptomycin 50 μg/ml). The flukes were transferred to fresh culture medium containing KTZ (1×10^{-4} M) for 2 h at 37°C. After the pre-incubation period, the flukes were transferred to fresh culture medium for 22 h at 37°C containing one of a number of drug and inhibitor combinations (Table 1). A stock solution of ketoconazole was initially prepared at a concentration of 1×10^{-1} M in methanol. A stock solution of nicotinamide adenine dinucleotide phosphate (NADPH) was initially prepared at a concentration of 1×10^{-3} M in distilled water. The concentration of KTZ used was chosen to be similar to those used in previous in vitro studies (Bourrie et al. 1996; Zhang et al. 2002; Dupuy et al. 2003; Virkel et al. 2006). The concentrations of TCBZ and TCBZ.SO used correspond to the maximum blood level of TCBZ.SO reached in vivo (13.3 μg/ml following a therapeutic dose of 10 mg/kg TCBZ in sheep; Hennessy et al. 1987). The two compounds were initially prepared as stock solutions in dimethyl sulphoxide and added to the culture medium to give a final solvent concentration of 0.1% (*v*/*v*). Controls were prepared by incubating whole flukes in NCTC 135 medium for 24 h at 37°C. Controls at 0 h were also prepared. After incubation, the flukes were fixed and processed for SEM. A minimum of four flukes were prepared for each treatment

Tissue preparation for SEM

Flukes were lightly flat-fixed for 1 h at room temperature in 4% (*w*/*v*) glutaraldehyde in 0.1 M sodium cacodylate buffer (pH 7.4) containing 3% (*w*/*v*) sucrose. The flukes were subsequently free-fixed in fresh fixative for a further 3 h at 4°C. The flukes were washed overnight at 4°C in 0.1 M sodium cacodylate buffer (pH 7.4) containing 3% (*w*/*v*) sucrose. After post-fixation in 1% osmium tetroxide for 1 h, the tissues were washed several times in fresh buffer, dehydrated through a series of ethanol, dried in hexamethyldisilazane, mounted on aluminium stubs, sputter-coated with gold-palladium and viewed in a FEI Quanta 200 scanning electron microscope operating at 10 keV.

Results

Given the large number (16) of experiments carried out in this study, a detailed description of surface changes observed for each one is not practicable. Instead, the text will focus on the main features of the response to each treatment and will be illustrated by appropriate micrographs. The surface architecture of the control specimens appeared normal. For images of normal morphology, the

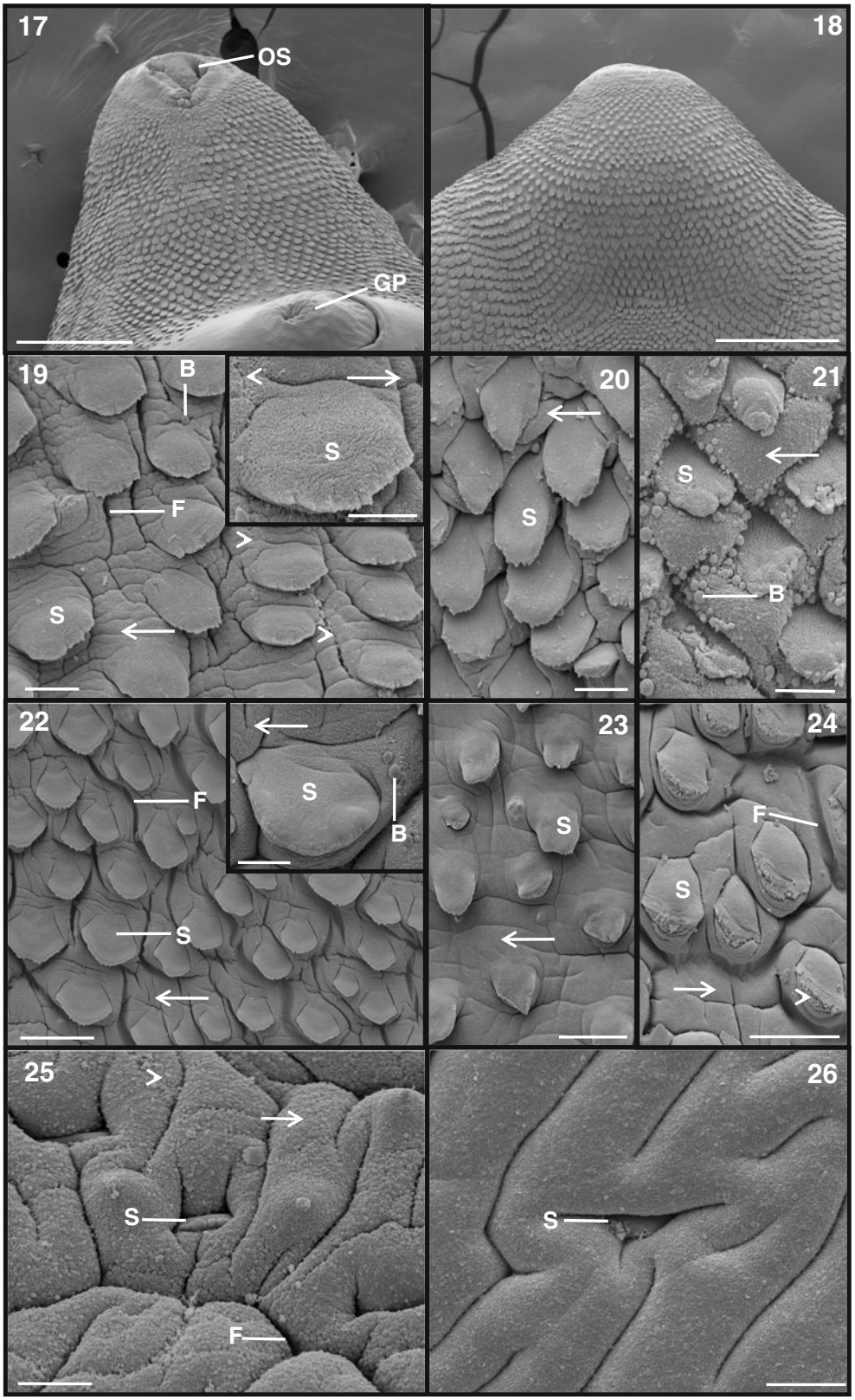
17
OS
GP
18
19
B
F
S
20
S
21
S
B
22
F
S
B
S
23
S
24
F
S
25
S
F
26
S

Figs. 17–26 Scanning electron micrographs (SEMs) of the tegumental surface of the liver fluke, *F. hepatica* (Cullompton isolate) following 24 h in vitro treatment with KTZ + NADPH + TCBZ

17 A low-power image of the ventral surface of the oral cone region. *OS* oral sucker, *GP* gonopore; *bar* 400 µm

18 Dorsal surface of the oral cone region; *bar* 400 µm

19 A high magnification image of the ventral surface of the apical cone region showing swelling (*arrow*), furrowing (*F*) and blebbing (*B*) of the tegumental surface. Patches of roughened tegument (*arrow heads*) were also observed; *bar* 20 µm. *Inset* highlights the swelling (*arrow*) and roughening (*arrow head*) of the tegument surrounding the spines (*S*); *bar* 10 µm

20 A high-power image of the dorsal surface of the apical cone region showing the swelling (*arrow*) of the tegument between the spines (*S*); *bar* 20 µm

21 Dorsal surface of the apical cone region highlighting swelling (*arrow*) and blebbing (*B*) of the interspinal tegument. *S* spine; *bar* 10 µm

22 Ventral surface of the midbody region showing swelling (*arrow*) and furrowing (*F*) of the tegument between the spines (*S*); *bar* 50 µm. *Inset* highlights swelling (*arrow*) and blebbing (*B*) of the interspinal tegument. *S* spine; *bar* 20 µm

23 A high magnification image of the dorsal surface of the midbody region showing slight swelling (*arrow*) of the interspinal tegument. *S* spine; *bar* 50 µm

24 Dorsal surface of the midbody region showing swelling (*arrow*) and furrowing (*F*) of the interspinal tegument. The spinelets have broken off the spine tip, so that it appears to be frayed (*arrow head*). *S* spine; *bar* 50 µm

25 Ventral surface of the tail region showing swelling (*arrow*) and furrowing (*F*) of the tegument between the spines (*S*). The spines appear submerged due to the swelling of the tegument surrounding them. The tegument also appears roughened (*arrow head*) in places; *bar* 10 µm

26 A high-power image of the dorsal surface of the tail region showing swelling of the tegument between the spines. The spine (*S*) appears sunken due to the swelling of the tegument surrounding it; *bar* 10 µm

reader is referred to the paper by McConville et al. (2009b: Figs. 1–6).

Cullompton and Oberon isolates treated with KTZ

A predominantly normal morphology was observed in the apical cone region, in both the Cullompton and Oberon isolates (Figs. 1 and 2). In the anterior midbody region of the Oberon isolate, swelling of the interspinal tegument was observed on the ventral surface (Fig. 3). The dorsal surface was slightly more swollen, with swelling of the tegument seen between and covering the spines (Fig. 4). The Cullompton isolate was more swollen in the anterior midbody region than the Oberon isolate, particularly on the dorsal surface. The posterior midbody region showed swelling and furrowing of the interspinal tegument on both surfaces (Figs. 5 and 6). On the dorsal surface, the tegument covering the spines was also swollen and, at higher magnification, its surface assumed a roughened appearance; the swelling obscured the spinelets (Fig. 6 inset). The surface features of the Cullompton isolate were similar, although more spine disruption was observed. The dorsal surface of the tail region of both isolates had a predominantly normal morphology, although the ventral surface of the Oberon isolate showed swelling and furrowing of the interspinal tegument and patches of roughened tegument (Fig. 7). The tegument covering the spines was swollen and this completely enclosed the spinelets (Fig. 7 inset). On the ventral surface of the Cullompton isolate, swelling and furrowing of the tegument between the spines was observed and the spines appeared partially submerged by the swollen tegument surrounding them (Fig. 8).

Cullompton and Oberon isolates treated with KTZ + NADPH

The apical cone region of both the isolates exhibited slight swelling of the interspinal tegument (Figs. 9–12). In the midbody region, swelling and furrowing of the interspinal tegument was evident on both surfaces (Figs. 13 and 14). Swelling of the tegument covering the spines was observed, especially on the ventral surface (Fig. 14). In the Cullompton isolate, swelling of the tegument was generally more severe, especially that covering the spines. In the tail region, swelling and furrowing of the interspinal tegument was seen in the Oberon isolate (Fig. 15). This swelling was greater in the Cullompton isolate (Fig. 16 and 16 inset a), with isolated patches of blebbing observed at higher magnification (Fig. 16 inset b).

Cullompton isolate treated with TCBZ and TCBZ.SO

Descriptions of surface changes brought about by treatment with the two drugs have been published elsewhere and will not be repeated here. The surface changes observed in the present study match these descriptions. Therefore, the reader is referred to the paper by Halferty et al. (2009) for changes brought about by TCBZ and TCBZ.SO (Figs. 1B, 2A, D and 3B and Figs. 1C, 2B, e and 3C, respectively) and the paper by Toner et al. (2009, Figs. 1 and 2) for changes induced by TCBZ.SO. In summary, after incubation in TCBZ, the tegument was swollen in all areas of the fluke, but was particularly severe in the oral cone, anterior midbody and tail regions, which caused the spines to appear partially or totally submerged. Extensive blebbing of the surface tegument was observed in the midbody region, with patchy and localised blebbing evident in the tail region. After 24 h incubation in TCBZ.SO, swelling of the interspinal tegument was observed in the oral cone region. The spine tips appeared to be disrupted as the tegument covering the spines had engulfed the spinelets. The midbody region showed tegumental swelling and blebbing, although the blebs were in localised patches. In the tail

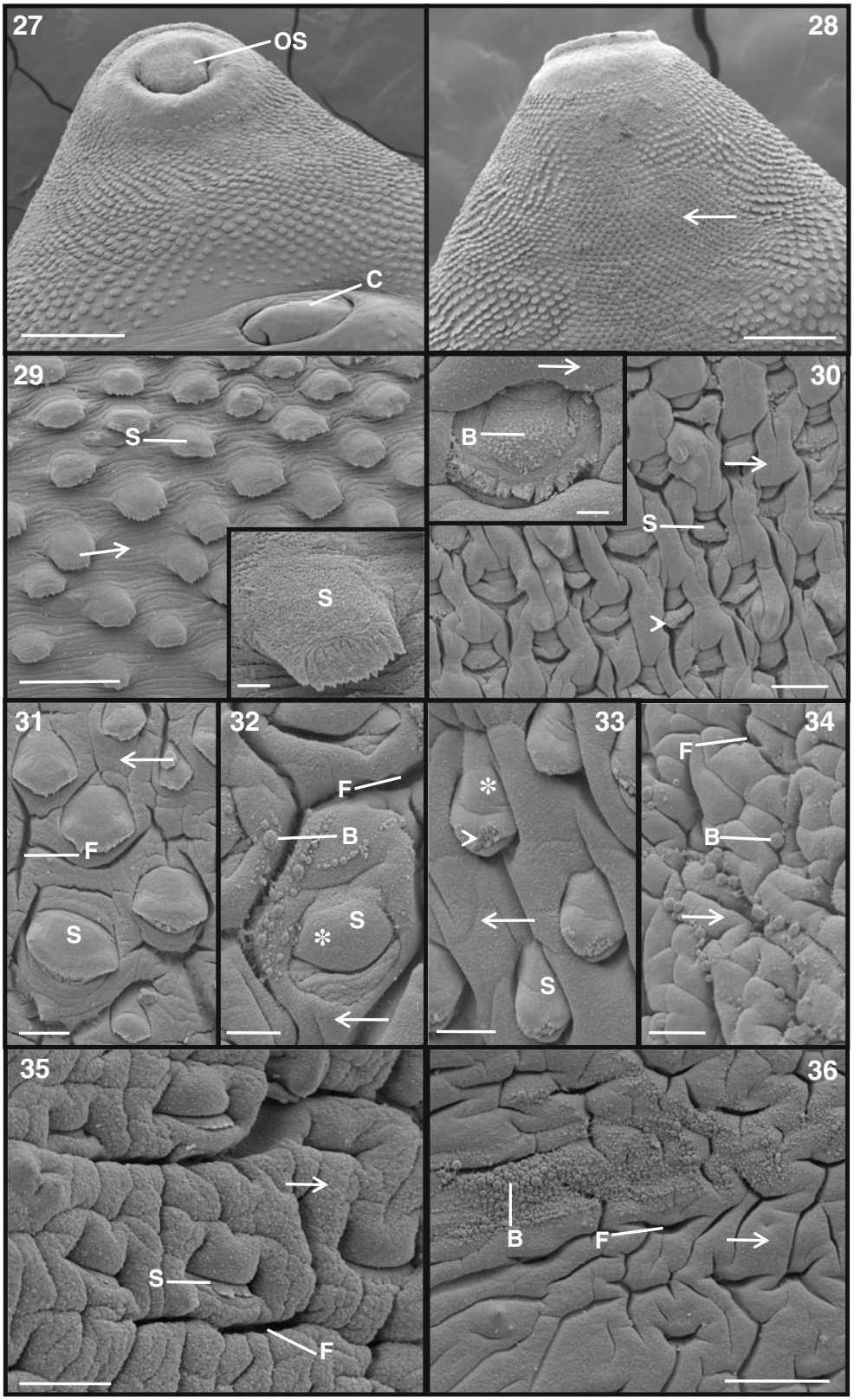
27
OS
C
28
29
S
S
B
30
S
31
F
S
32
F
B
S
33
S
34
F
B
35
S
F
36
B
F

◀**Figs. 27–36** Scanning electron micrographs (SEMs) of the tegumental surface of the liver fluke, *F. hepatica* (Cullompton isolate) following 24 h in vitro treatment with KTZ + NADPH + TCBZ.SO

27 A low-power image of the ventral surface of the oral cone region. *OS* oral sucker, *C* cirrus; *bar* 300 μm

28 Dorsal surface of the apical cone region showing areas of tegumental swelling (*arrow*); *bar* 300 μm

29 Image of the ventral surface of the apical cone region showing the slight swelling of the tegument between (*arrow*) and covering the spines (*S*); *bar* 50 μm. *Inset* shows a high-power image of a spine (*S*); *bar* 5 μm

30 Dorsal surface of the oral cone region showing swelling of the interspinal tegument (*arrow*). The tegument covering the spine has engulfed the spine tips (*arrow head*). *S*, spine; *bar* 20 μm. *Inset* shows swelling (*arrow*) of the tegument between the spines and blebbing (*B*) on the surface of the spine; *bar* 5 μm

31 Ventral surface of the midbody region showing swelling (*arrow*) and furrowing (*F*) of the interspinal tegument. The tegument covering the spines (*S*) is swollen; *bar* 20 μm

32 A high-power image of the ventral midbody surface showing swelling (*arrow*), furrowing (*F*) and blebbing (*B*) of the tegument between the spines (*S*). The tegument covering the spines appears swollen (*asterisk*); *bar* 20 μm

33 A high magnification image of the dorsal surface of the midbody region showing swelling of the interspinal tegument (*arrow*) and of the tegument covering the spines (*asterisk*). The spinelets have broken off the tip of the spine, so that the tip appears to be frayed (*arrow head*). *S* spine; *bar* 20 μm

34 Dorsal surface of the midbody region showing swelling (*arrow*), furrowing (*F*) and blebbing (*B*) of the interspinal tegument. The swelling is so severe that no spines are visible; *bar* 20 μm

35 Ventral surface of the tail region showing swelling (*arrow*) and furrowing (*F*) of the interspinal tegument. The spines (*S*) appear sunken due to the swelling of the tegument surrounding them; *bar* 20 μm

36 Dorsal surface of the tail region showing swelling (*arrow*), furrowing (*F*) and blebbing (*B*) of the interspinal tegument. The tegumental swelling is so severe that the spines are totally submerged and not visible; *bar* 50 μm

region, the tegument was swollen with patches of quite extensive blebbing visible.

Cullompton isolate treated with KTZ + NADPH + TCBZ

After 24 h incubation, the tegument on both surfaces of the apical cone region was swollen (Figs. 17 and 18). On the ventral surface, the tegument was furrowed with isolated blebs present on the surface (Fig. 19). The tegument assumed a roughened appearance, but the spines retained a relatively normal morphology (Fig. 19 inset). On the dorsal surface, swelling of the interspinal tegument was observed (Fig. 20), with other areas of more severe tegumental swelling and blebbing (Fig. 21). In the ventral midbody region, the tegument was swollen and furrowed (Fig. 22), with blebbing evident at higher magnification (Fig. 22 inset). On the dorsal surface of this region, only slight swelling of the tegument was observed in some areas (Fig. 23), although in other areas the tegument was more severely swollen and furrowed. In these areas, the spinelets had broken off, so that the spine tips appeared frayed (Fig. 24). The ventral surface of the tail region showed swelling and furrowing of the tegument and had a 'roughened' appearance (Fig. 25). The dorsal surface of the tail region showed general swelling of the tegument between the spines (Fig. 26). On both surfaces, the spines appeared submerged by the swollen tegument surrounding them (Figs. 25 and 26).

Cullompton isolate treated with KTZ + NADPH + TCBZ.SO

The ventral surface of the apical cone region retained a relatively normal morphology at low magnification (Fig. 27), although swelling of the interspinal tegument was visible at low magnification on the dorsal surface (Fig. 28). At higher magnification, slight swelling of the tegument between (Fig. 29) and covering (Fig. 29 inset) the spines was observed. On the dorsal surface, more severe swelling of the interspinal tegument was observed (Fig. 30). At higher magnification, the spines appeared sunken due to tegumental swelling and blebbing was visible on the tegumental covering of the spines (Fig. 30 inset). The tegument on the ventral surface of the midbody region was swollen between and covering the spines and was furrowed in places (Fig. 31). In some areas of the ventral midbody, blebs were present on the tegumental surface (Fig. 32). On the dorsal surface in the midbody region, the tegument between and covering the spines was swollen, and the spinelets had broken off, giving the spine tips a frayed appearance (Fig. 33). Other regions showed more severe swelling and blebbing, and the tegument was so swollen that no spines were visible (Fig. 34). On the ventral surface in the tail region, the tegument was swollen both between and covering the spines, and furrowing was also evident (Fig. 35). The dorsal surface showed more severe swelling between the spines; furrowing and blebbing of the tegument were also observed (Fig. 36). In the tail region, spines were barely visible due to the swelling of the tegument surrounding them (Figs. 35 and 36).

Oberon isolate treated with TCBZ and TCBZ.SO

Descriptions of surface changes brought about by treatment with the two drugs have been published elsewhere and will not be repeated here. The surface changes observed in the present study are similar to those described by Devine et al. (2009: Fig. 4) and Walker et al. (2004: Figs. 17–24) for changes following treatment with TCBZ and TCBZ.SO, respectively. In summary, following incubation in TCBZ for 24 h, a predominantly normal morphology was observed in the apical cone region. In the midbody region,

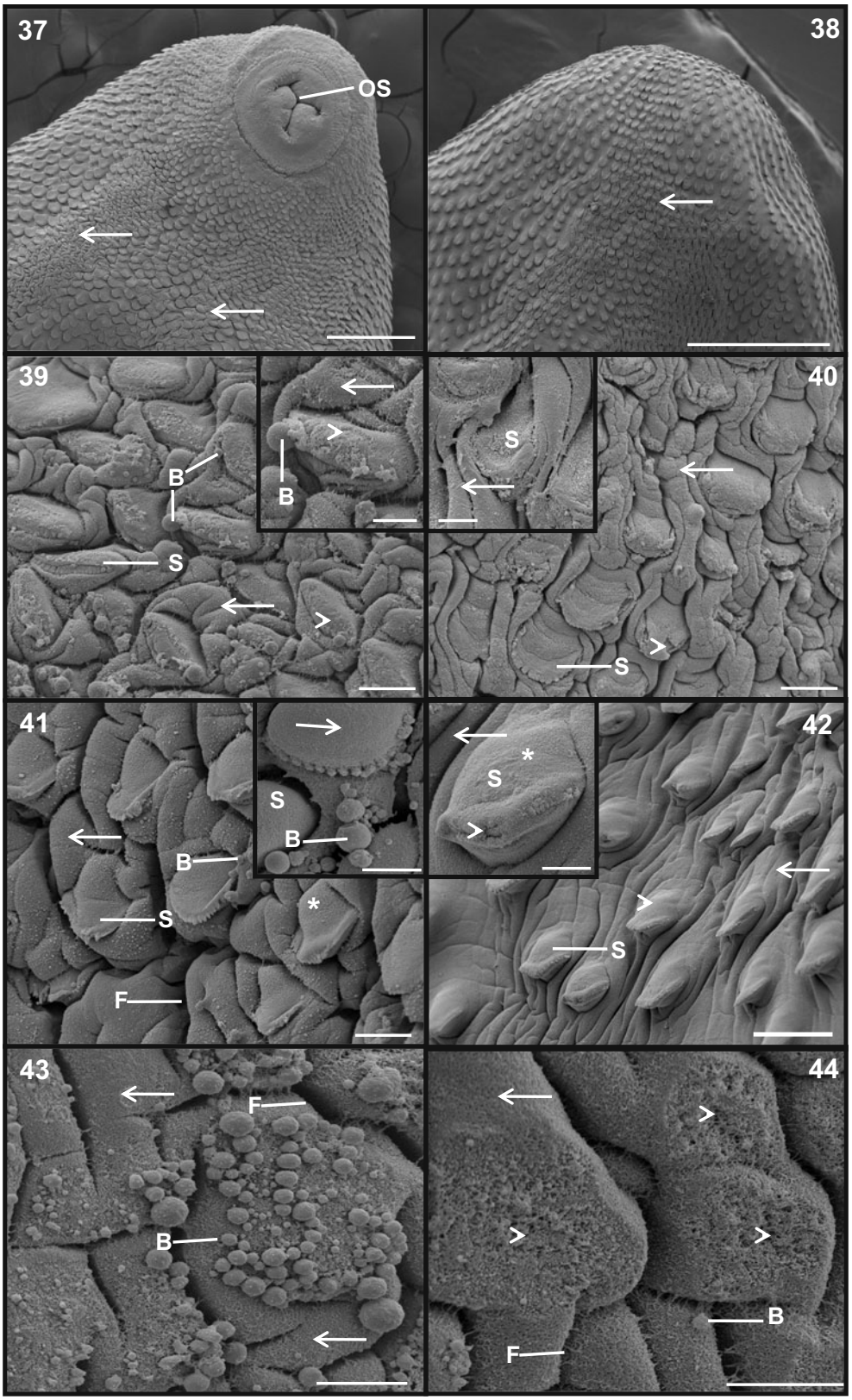
37
OS
38
39
B
B
S
40
S
S
41
S
B
B
S
F
*
42
S
*
S
43
F
B
44
B
F

Figs. 37–44 Scanning electron micrographs (SEMs) of the tegumental surface of the liver fluke, *F. hepatica* (Oberon isolate) following 24 h in vitro treatment with KTZ + NADPH + TCBZ
37 Ventral surface of the apical cone region showing areas of tegumental swelling (*arrows*). *OS* oral sucker; *bar* 300 µm
38 A low-power image of the dorsal surface of the oral cone region showing areas of tegumental swelling (*arrow*); *bar* 400 µm
39 A high-power image of the ventral surface of the oral cone region showing extensive swelling (*arrow*) of the interspinal tegument and areas of blebbing (*B*) on the tegumental surface and spine tips. Loss of apical plasma membrane (*arrow head*) on the spines was also seen. *S*, spine; *bar* 20 µm. *Inset* shows a higher magnification image of the swelling of the tegument (*arrow*) between the spines and blebbing (*B*) associated with the spine tips. Sloughing of the apical plasma membrane (*arrow head*) can also be seen on the spines. *Inset* 10 µm
40 Dorsal surface of the oral cone region showing swelling (*arrow*) of the tegument between the spines (*S*). Sloughing of the tegument (*arrow head*) covering the spines is also evident; *bar* 20 µm. *Inset* shows a high-power image of a spine (*S*) which appears sunken due to the swelling of the tegument surrounding it (*arrow*); *bar* 10 µm
41 Ventral surface of the midbody region showing swelling of the tegument covering (*asterisk*) and between (*arrow*) the spines (*S*). Blebbing (*B*) and furrowing (*F*) of the tegument can also be seen; *bar* 20 µm. *Inset* shows a high-power image of the severe swelling of the tegument covering (*arrow*) the spine (*S*) and blebbing (*B*) on the tegumental surface; *bar* 10 µm
42 Dorsal surface of the midbody region showing swelling of the tegument between (*arrow*) and covering (*arrow head*) the spines (*S*); *bar* 50 µm. *Inset* shows a high magnification image of a spine (*S*) showing swelling of the tegument around (*arrow*) and covering (*asterisk*) it. The swelling has obscured the spinelets (*arrow head*); *bar* 10 µm
43 Dorsal surface of the tail region showing swelling (*arrows*), furrowing (*F*) and extensive blebbing (*B*) of the tegumental surface. The tegumental swelling is so severe that no spines are visible; *bar* 10 µm
44 A high-power image of the dorsal surface of the tail region showing extensive swelling (*arrow*) of the tegument, blebbing (*B*) and patches of sloughing of the apical plasma membrane (*arrow heads*). The tegumental swelling is so severe that the spines are totally submerged and not visible; *bar* 10 µm

general swelling of the interspinal tegument was observed. The tail region showed localised areas of disruption, with severe swelling and furrowing of the tegument. The tegument was so swollen in places that the spines were partially or totally submerged. Following 24 h incubation in TCBZ.SO, the tegument was swollen in all body regions, especially towards the anterior end of the fluke. Blebbing was quite extensive in the midbody region, and occurred in patches in the oral cone and tail regions. Microvillus-like projections caused the tegument to assume a roughened appearance in the midbody and tail regions.

Oberon isolate treated with KTZ + NADPH + TCBZ

At low magnification, areas of tegumental swelling were observed on both surfaces of the apical cone region (Figs. 37 and 38). In the oral cone region, sloughing of the apical plasma membrane covering the spines was observed on both surfaces (Figs. 39 and 40); blebbing was also seen on the ventral surface (Fig. 39). On the ventral surface in the midbody region, swelling, furrowing and blebbing of the interspinal tegument was evident (Fig. 41). At higher magnification, swelling of the tegument covering the spines and blebbing of the interspinal tegument were seen (Fig. 41 inset). On the dorsal surface, the tegument was swollen both between and covering the spines (Fig. 42); the latter served to obscure the spinelets (Fig. 42 inset). The ventral surface of the tail region retained a relatively normal morphology, with only general swelling observed. The dorsal surface showed severe swelling, blebbing and furrowing of the tegument (Fig. 43). On this surface, there were areas where the apical plasma membrane had been lost (Fig. 44). No spines were visible due to the severe swelling of the tegument surrounding them (Figs. 43 and 44).

Oberon isolate treated with KTZ + NADPH + TCBZ.SO

The ventral surface of the apical cone region showed a predominantly normal morphology at low magnification (Fig. 45), although the dorsal surface showed areas of tegumental swelling (Fig. 46). After 24-h incubation, the tegument on the ventral surface of the apical cone region was slightly swollen (Fig. 47). At higher magnification, it was seen that the spinelets were beginning to break down and the tegument had started to split at their bases (Fig. 47 inset). On the dorsal surface, severe swelling of the tegument between the spines caused the spines to appear sunken into the tegument (Fig. 48). Swelling of the tegument covering the spines obscured the spinelets (Fig. 48) and, at higher magnification, blebbing could be seen on the spine tips (Fig. 48 inset). In the midbody region, swelling, furrowing and blebbing of the tegument were observed on the ventral surface (Fig. 49); swelling of the tegument covering the spines was also visible (Fig. 49 inset). On the dorsal surface, the tegument covering and between the spines was swollen and furrowing and blebbing were visible, with patches of tegumental roughening (Fig. 50). At higher magnification, blebs were observed on the tegument covering the spines and, at the spine tips, some of the spinelets had broken off (Fig. 50 inset). The ventral surface of the tail region showed swelling, furrowing and roughening of the tegument between the spines (Fig. 51); on the dorsal surface, swelling and furrowing of the interspinal tegument was evident (Fig. 52).

The main changes brought about by drug action and the relative severity of these changes are summarised in Tables 2 and 3.

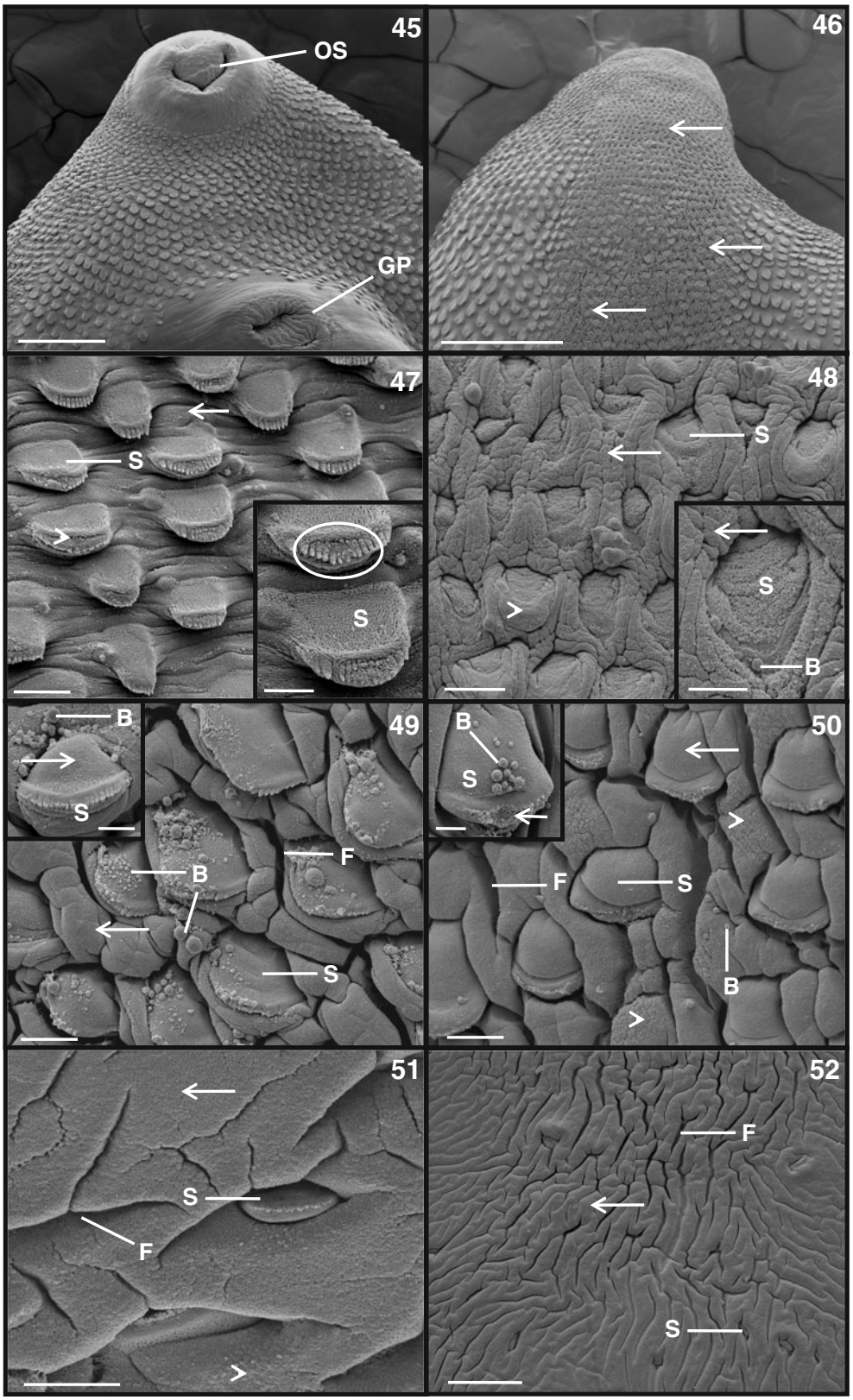
45
OS
GP
46
47
S
S
48
S
S
B
49
B
S
F
B
S
50
B
S
F
S
B
51
S
F
52
F
S

Figs. 45–52 Scanning electron micrographs (SEMs) of the tegumental surface of the liver fluke, *F. hepatica* (Oberon isolate) following 24 h in vitro treatment with KTZ + NADPH + TCBZ.SO
45 A low-power image of the ventral surface of the apical cone region. *OS* oral sucker, *GP* gonopore; *bar* 300 µm
46 Dorsal surface of the oral cone region highlighting areas of tegumental swelling between the spines (*arrows*); *bar* 400 µm
47 A high-power image of the ventral surface of the oral cone region, showing swelling (*arrow*) of the tegument between the spines (*S*) and disruption to the spinelets, together with splitting of the tegument at their bases (*arrow head*); *bar* 20 µm. *Inset* shows a higher power image of the spines (*S*) and the breakdown of the spinelets (*circle*); *bar* 10 µm
48 Image of the dorsal surface of the oral cone region showing spines (*S*) which appear sunken due to the swelling (*arrow*) of the tegument between them. The tegument covering the spines is swollen, too, which has obscured the spinelets (*arrow head*); *bar* 20 µm. *Inset* is a high-power image of the tegumental surface, highlighting the extensive swelling (*arrow*) between the spines (*S*) and blebbing (*B*) associated with the spine tips; *bar* 10 µm
49 Ventral surface of the midbody region showing swelling (*arrow*) and furrowing (*F*) of the tegumental surface. Blebbing (*B*) was associated with the tegument covering and between the spines (*S*); *bar* 20 µm. *Inset* shows a high-power image of the swelling (*arrow*) of the tegument covering the spine (*S*) and blebbing (*B*) of the tegumental surface; *bar* 10 µm
50 Dorsal surface of the midbody region showing swelling of the tegument covering (*arrow*) and between the spines (*S*), also tegumental furrowing (*F*) and blebbing (*B*). The tegument assumes a roughened appearance (*arrow heads*) in places; *bar* 20 µm. *Inset* highlights blebbing (*B*) on the surface of a spine (*S*). Some of the spinelets have broken off the spine tip (*arrow*); *bar* 20 µm
51 A high-power image of the ventral surface of the tail region showing the swelling (*arrow*) and furrowing (*F*) of the tegument between the spines (*S*). The spines are partially sunken by the swelling of the tegument surrounding them. The tegument also assumes a roughened appearance (*arrow head*) in places; *bar* 50 µm
52 Dorsal surface of the tail region showing swelling (*arrow*) and furrowing (*F*) of the tegument. The spines (*S*) appear sunken due to the swelling of the tegument around them; *bar* 10 µm

Discussion

The results of this investigation have demonstrated that KTZ, a CYP 450 inhibitor, can potentiate the action of TCBZ and TCBZ.SO against the TCBZ-resistant Oberon fluke isolate. While treatment with TCBZ and (more particularly) TCBZ.SO caused greater disruption of the Cullompton isolate, potentiation of drug action was only observed with the Oberon isolate. Incubation in KTZ alone or KTZ + NADPH caused limited disruption to the surface features of both isolates. After incubation in KTZ for 24 h, slight swelling and furrowing of the tegument was observed in both isolates, and the tegument covering the spines was also swollen. Swelling was more widespread in the Cullompton than Oberon isolate. KTZ + NADPH treatment again resulted in slight swelling and furrowing of the tegument, with the swelling to the tegument around the spines being more severe than that seen with KTZ alone. The Cullompton isolate again was more disrupted than the Oberon isolate, but the level of disruption for the two isolates with these treatments was not significant.

In the Oberon isolate, TCBZ alone caused general tegumental swelling and there was some roughening of the surface in the posterior half of the body due to the presence of microvillus-like projections. Combining TCBZ with KTZ resulted in severe swelling of the tegument, tegumental blebbing and loss of the apical plasma membrane. TCBZ.SO caused greater tegumental disruption to the Oberon isolate than TCBZ, as there was more extensive swelling and blebbing of the tegument. The addition of KTZ to the incubation medium increased the level of disruption seen with TCBZ.SO alone: extensive swelling and furrowing of the tegument, roughening of the tegumental surface and tegumental sloughing were seen, along with spine disruption. This took the form of swelling of its tegumental covering and damage to the spinelets. Therefore, with the Oberon isolate, incubation in TCBZ.SO alone resulted in greater disruption than TCBZ; co-incubation with KTZ lead to more disruption with both drugs; and KTZ + NADPH + TCBZ.SO was the most disruptive of all treatments.

Following incubation in TCBZ, with the Cullompton isolate, there was widespread swelling, furrowing and blebbing of the tegumental surface. On the addition of KTZ to the incubation medium, the level of disruption observed was similar to that seen with the drug alone. TCBZ.SO treatment alone caused more severe swelling and blebbing of the tegumental surface in the TCBZ-susceptible isolate than the TCBZ-resistant Oberon isolate. This disruption increased slightly with the addition of KTZ and NADPH to the incubation medium. Treatment with TCBZ and TCBZ.SO on their own caused a similar level of disruption; co-incubation with KTZ did not exacerbate the disruption caused by TCBZ alone, but did slightly accentuate that induced by TCBZ.SO.

The results indicate that the inhibition of a drug metabolism pathway has a greater effect on a TCBZ-resistant isolate than a TCBZ-susceptible one. It has been shown that the capacity of the TCBZ-resistant Sligo isolate to metabolise TCBZ to TCBZ.SO is significantly higher than that of the TCBZ-susceptible Cullompton isolate (Alvarez et al. 2005). Similarly, the TCBZ-resistant Sligo isolate's ability to metabolise TCBZ.SO to TCBZ.SO_2 is greater than that of the TCBZ-susceptible isolate (Robinson et al. 2004). This may be due to the fact that the TCBZ-resistant isolates are more reliant on these pathways, possibly due to an over-expression of the CYP 450 enzyme, so inhibition of the pathway leaves them more sensitive to drug action. The metabolism of the TCBZ-susceptible isolate is unaltered, so inhibiting its metabolic pathways

Table 2 Oberon isolate of *Fasciola hepatica*. Summary of surface changes following different drug treatments

Disruption	Treatment					
	KTZ	KTZ + NADPH	KTZ + NADPH + TCBZ	TCBZ	TCBZ.SO	KTZ + NADPH + TCBZ.SO
Swelling of tegument between spines	+	++	+++	+	++	+++
Swelling of tegument covering spines	+	+	++	−	−	++
Disruption to spines	+	+	+	+	−	++
Furrowing of tegument	+	+	++	−	−	++
Blebbing	−	−	++	−	++	++
Roughening of the tegument	−	−	−	−	−	++
Microvillus-like projections	−	−	−	+	+	−
Sloughing of the apical plasma membrane	−	−	++	−	−	+
Totals	4	5	12	3	5	14

− no noticeable disruption, + general/mild disruption; ++ severe disruption, +++ very severe disruption, *KTZ* ketoconazole, *NADPH* nicotinamide adenine dinucleotide phosphate, *TCBZ* triclabendazole, *TCBZ.SO* triclabendazole sulphoxide

has less of an effect on it and, as a result, there is little or no potentiation of drug action.

Other morphological and biochemical studies involving different metabolic inhibitors have shown that the inhibition of a drug metabolism pathway has a comparatively greater effect on two TCBZ-resistant isolates than a TCBZ-susceptible one (Alvarez et al. 2005; Devine et al. 2009, 2010a, b). This is a potentially significant finding, as it suggests that TCBZ-resistant isolates of different geographical origin respond in a similar way to metabolic inhibition. Of the two CYP450 inhibitors used (KTZ and PB), KTZ appeared to cause the greater disruption, in the sense that there was sloughing of the apical plasma membrane, which would lead to loss of the tegument and cause widespread disruption of the internal tissues. Enhancement of oxidative metabolism may contribute to the mechanism of resistance within TCBZ-resistant isolates (Alvarez et al. 2005; Devine et al. 2009, 2010a, b), but it may not be the only process involved, as other evidence points to the mechanism as being multi-factorial. For example, the accumulation of TCBZ and TCBZ.SO has been shown to be significantly reduced in the TCBZ-resistant Sligo isolate (Alvarez et al. 2005; Mottier et al. 2006b). Reduced drug uptake would lower the effective concentrations of TCBZ metabolites within the fluke and this, combined with more rapid metabolism and inactivation, would reduce their ability to reach the target molecule for drug action.

A number of studies have demonstrated that co-administration of metabolic inhibitors can enhance the pharmacokinetic profile of antiparasitic drugs and so

Table 3 Cullompton isolate of *Fasciola hepatica*. Summary of surface changes following different drug treatments

Disruption	Treatment					
	KTZ	KTZ + NADPH	KTZ + NADPH + TCBZ	TCBZ	TCBZ.SO	KTZ + NADPH + TCBZ.SO
Swelling of tegument between spines	++	+	++	+++	++	+++
Swelling of tegument covering spines	+	++	+	+	−	++
Disruption to spines	+	+	−	−	+	+
Furrowing of tegument	+	+	−	++	++	++
Blebbing	−	+	++	++	++	++
Roughening of the tegument	−	−	++	−	−	−
Microvillus-like projections	−	−	−	−	−	−
Sloughing of the apical plasma membrane	−	−	−	−	−	−
Totals	5	6	7	8	7	10

− no noticeable disruption, + general/mild disruption, ++ severe disruption, +++ very severe disruption, *KTZ* ketoconazole, *NADPH* nicotinamide adenine dinucleotide phosphate, *TCBZ* triclabendazole, *TCBZ.SO* triclabendazole sulphoxide

increase their bioavailability: studies not just on benzimidazoles (Luder et al. 1986; Bekhti and Pirotte 1987; Wen et al. 1996; Lanusse and Prichard 1991, 1992a, b; Lanusse et al. 1992; López-García et al. 1998; McKellar et al. 2002; Sánchez et al. 2002; Merino et al. 2003a, b), but on other compounds such as macrocyclic lactones (Hugnet et al. 2007; Alvinerie et al. 2008), the anti-schistosomal drug, praziquantel (Diekmann et al. 1989; Ridtitid et al. 2007) and the anti-malarial, mefloquine (Ridtitid et al. 2005; Wisedpanichkij et al. 2009). The potentiation of drug availability observed has lead a number of workers to propose the use of such drug combinations as a strategy to deal with drug resistance (Lanusse and Prichard 1993; Lanusse et al. 1995; Benchaoui and McKellar 1996; Dupuy et al. 2003; Sánchez-Bruni et al. 2005; Alvinerie et al. 2008; Wisedpanichkij et al. 2009).

In conclusion, this study has shown that it is possible to modulate the susceptibility of a TCBZ-resistant fluke isolate and convert it to a more TCBZ-susceptible state by combining it with the CYP 450 inhibitor, ketoconazole. With no new anthelmintics being developed for *F. hepatica*, the use of inhibitor-drug combinations may improve the action of TCBZ, which still remains the most effective anti-fluke drug. Modulating drug metabolism within both the host and the parasite represents a possible avenue to maintain drug activity, especially against TCBZ-resistant isolates. As mentioned previously, co-administration of KTZ with TCBZ leads to a higher peak plasma concentration of TCBZ.SO than that measured following TCBZ treatment alone and so enhances the bioavailability of TCBZ.SO in sheep (Virkel et al. 2009). In turn, this may lead to a greater efficacy against fluke. To test this idea, an in vivo study in the laboratory rat model has been carried out to monitor morphological changes over a 4-day period resulting from KTZ + TCBZ combination treatment; the results of this experiment will be published separately.

Acknowledgements This investigation was supported by a DARDNI Postgraduate Studentship to Catherine Devine. It was also partially supported by a grant from the European Union (DELIVER grant, no. FOOD-CT-200X-023025) and by a BBSRC/Defra grant (C00082X/1).

References

Alvarez LI, Solana HD, Mottier ML, Virkel GL, Fairweather I, Lanusse CE (2005) Altered drug influx/efflux and enhanced metabolic activity in triclabendazole-resistant liver flukes. Parasitology 131:501–510

Alvinerie M, Dupuy J, Eeckhoutte C, Sutra JF, Kerboeuf D (2001) In vitro metabolism of moxidectin in *Haemonchus contortus* adult stages. Parasitol Res 87:702–704

Alvinerie M, Dupuy J, Kiki-Mvouaka S, Sutra J-F, Lespine A (2008) Ketoconazole increases the plasma levels of ivermectin in sheep. Vet Parasitol 157:117–122

Bekhti A, Pirotte J (1987) Cimetidine increases serum mebendazole concentrations: implications for treatment of hepatic hydatid cysts. Br J Clin Pharmacol 24:390–392

Benchaoui HA, McKellar QA (1996) Interaction between fenbendazole and piperonyl butoxide: pharmacokinetic and pharmacodynamic implications. J Pharm Pharmacol 48:753–759

Bourrie M, Meunier V, Berger Y, Fabre G (1996) Cytochrome P450 isoform inhibitors as a tool for the investigation of metabolic reactions catalyzed by human liver microsomes. J Pharmacol Exp Ther 277:321–332

Brennan GP, Fairweather I, Trudgett A, Hoey E, McCoy M, McConville M, Meaney M, Robinson M, McFerran N, Ryan L, Lanusse C, Mottier L, Alvarez L, Solana H, Virkel G, Brophy PM (2007) Understanding triclabendazole resistance. Exp Mol Pathol 82:104–109

Cvilink V, Skálová L, Szotáková B, Lamka J, Kostiainen R, Ketola RA (2008) LC-MS-MS identification of albendazole and flubendazole metabolites formed *ex vivo* by *Haemonchus contortus*. Anal Bioanal Chem 391:337–343

Cvilink V, Szotáková B, Krížová V, Lamka J, Skálová L (2009) Phase I biotransformation of albendazole in lancet fluke (*Dicrocoelium dendriticum*). Res Vet Sci 86:49–55

Devine C, Brennan GP, Lanusse CE, Alvarez LI, Trudgett A, Hoey E, Fairweather I (2009) Effect of the metabolic inhibitor, methimazole on the drug susceptibility of a triclabendazole-resistant isolate of *Fasciola hepatica*. Parasitology 136:183–192

Devine C, Brennan GP, Lanusse CE, Alvarez LI, Trudgett A, Hoey E, Fairweather I (2010a) Inhibition of cytochrome P450-mediated metabolism enhances *ex vivo* susceptibility of *Fasciola hepatica* to triclabendazole. Parasitology (in press)

Devine C, Brennan GP, Lanusse CE, Alvarez LI, Trudgett A, Hoey E, Fairweather I (2010b) Potentiation of triclabendazole sulphoxide-induced tegumental disruption by methimazole in a triclabendazole-resistant isolate of *Fasciola hepatica*. Parasitol Res (in press)

Diekmann HW, Schneidereit M, Overbosch D (1989) Inhibitory effects of cimetidine, ketoconazole and miconazole on the metabolism of praziquantel. Acta Leidens 57:217–228

Dupuy J, Larrieu G, Sutra JF, Lespine A, Alvinerie M (2003) Enhancement of moxidectin bioavailability in lamb by a natural flavonoid: quercetin. Vet Parasitol 112:337–347

Fairweather I, Threadgold LT, Hanna REB (1999) Development of *Fasciola hepatica* in the mammalian host. In: Dalton JP (ed) Fasciolosis. CAB International, Wallingford, pp 47–111

Gotoh O (1998) Divergent structures of *Caenorhabditis elegans* cytochrome P450 genes suggest the frequent loss and gain of introns during the evolution of nematodes. Mol Biol Evol 15:1447–1459

Halferty L, Brennan GP, Hanna REB, Edgar HW, Meaney MM, McConville M, Trudgett A, Hoey L, Fairweather I (2008) Tegumental surface changes in juvenile *Fasciola hepatica* in response to treatment *in vivo* with triclabendazole. Vet Parasitol 155:49–58

Halferty L, Brennan GP, Trudgett A, Hoey EM, Fairweather I (2009) The relative activity of triclabendazole metabolites against the liver fluke, *Fasciola hepatica*. Vet Parasitol 159:126–138

Hanna REB, Edgar HWJ, McConnell S, Toner E, McConville M, Brennan GP, Devine C, Flanagan A, Halferty L, Meaney M, Shaw L, Moffett D, McCoy M, Fairweather I (2010) *Fasciola hepatica*: histological changes in the reproductive structures of triclabendazole (TCBZ)-sensitive and TCBZ-resistant flukes collected from experimentally infected sheep one to four days

after treatment with TCBZ and the related benzimidazole derivative, Compound Alpha. Vet Parasitol 168:240–254

Hennessy DR, Lacey E, Steel JW, Prichard RK (1987) The kinetics of triclabendazole disposition in sheep. J Vet Pharmacol Ther 10:64–72

Hugnet C, Lespine A, Alvinerie M (2007) Multiple oral dosing of ketoconazole increases dog exposure to ivermectin. J Pharm Pharmaceut Sci 10:311–318

Keiser J, Utzinger J, Vennerstrom JL, Dong Y, Brennan GP, Fairweather I (2007) Activity of artemether and OZ78 against triclabendazole-resistant *Fasciola hepatica*. Trans R Soc Trop Med Hyg 101:1219–1222

Kerboeuf D, Soubieux D, Guilluy R, Brazier JL, Riviere JL (1995) In vivo metabolism of aminopyrine by the larvae of the helminth *Heligmosomoides polygyrus*. Parasitol Res 81:302–304

Kotze AC (1997) Cytochrome P450 monooxygenase activity in *Haemonchus contortus* (Nematoda). Int J Parasitol 27:33–40

Kotze AC (1999) Peroxide-supported in-vitro cytochrome P450 activities in *Haemonchus contortus*. Int J Parasitol 29:389–396

Kotze AC (2000) Oxidase activities in macrocyclic-resistant and -susceptible *Haemonchus contortus*. J Parasitol 86:873–876

Kotze AC, Dobson RJ, Chandler D (2006) Synergism of rotenone by piperonyl butoxide in *Haemonchus contortus* and *Trichostrongylus colubriformis* in vitro: potential for drug-synergism through inhibition of nematode oxidative detoxification pathways. Vet Parasitol 136:275–282

Lanusse CE, Prichard RK (1991) Enhancement of the plasma concentration of albendazole sulfoxide in sheep following coadministration of parenteral netobimin and liver oxidase inhibitors. Res Vet Sci 51:306–312

Lanusse CE, Prichard RK (1992a) Effects of methimazole on the kinetics on netobimin metabolites in cattle. Xenobiotica 22:115–123

Lanusse CE, Prichard RK (1992b) Methimazole increases the plasma concentrations of the albendazole metabolites of netobimin in sheep. Biopharm Drug Dispos 13:95–103

Lanusse CE, Prichard RK (1993) Clinical pharmacokinetics and metabolism of benzimidazole anthelmintics in ruminants. Drug Metab Rev 25:235–279

Lanusse CE, Gascon L, Prichard RK (1992) Methimazole-mediated modulation of netobimin biotransformation in sheep: a pharmacokinetic assessment. J Vet Pharmacol Ther 15:267–274

Lanusse CE, Gascon LH, Prichard RK (1995) Influence of the antithyroid compound methimazole on the plasma disposition of fenbendazole and oxfendazole in sheep. Res Vet Sci 58:222–226

López-García ML, Torrado S, Torrado S, Martínez AR, Bolás F (1998) Methimazole-mediated enhancement of albendazole oral bioavailability and anthelmintic effects against parenteral stages of *Trichinella spiralis* in mice: the influence of the dose-regime. Vet Parasitol 75:209–219

Luder PJ, Siffert B, Witassek F, Meister F, Bircher J (1986) Treatment of hydatid disease with high oral doses of mebendazole. Long-term follow-up of plasma mebendazole levels and drug interactions. Eur J Clin Pharmacol 31:443–448

McConville M, Brennan GP, McCoy M, Castillo R, Hernández-Campos A, Ibarra F, Fairweather I (2006) Adult triclabendazole-resistant *Fasciola hepatica*: surface and subsurface tegumental responses to *in vitro* treatment with the sulphoxide metabolite of the experimental fasciolicide compound alpha. Parasitology 133:195–208

McConville M, Brennan GP, Flanagan A, Edgar HWJ, Hanna REB, McCoy M, Gordon AW, Castillo R, Hernández-Campos A, Fairweather I (2009a) An evaluation of the efficacy of compound alpha and triclabendazole against two isolates of *Fasciola hepatica*. Vet Parasitol 162:75–88

McConville M, Brennan GP, Flanagan A, Hanna REB, Edgar HWJ, Castillo R, Hernández-Campos A, Fairweather I (2009b) Surface changes in adult *Fasciola hepatica* following treatment in vivo with the experimental fasciolicide, compound alpha. Parasitol Res 105:757–767

McCoy MA, Fairweather I, Brennan GP, Kenny JM, Forbes AF (2005) The efficacy of nitroxynil and triclabendazole administered synchronously against juvenile triclabendazole-resistant *Fasciola hepatica* in sheep. Res Vet Sci 78(Suppl A):33

McKellar QA, Gokbulut C, Muzandu K, Benchaoui H (2002) Fenbendazole pharmacokinetics, metabolism, and potentiation in horses. Drug Metab Dispos 30:1230–1239

Meaney M, Allister J, McKinstry B, McLaughlin K, Brennan GP, Forbes AB, Fairweather I (2006) *Fasciola hepatica*: morphological effects of a combination of triclabendazole and clorsulon against mature fluke. Parasitol Res 99:609–621

Meaney M, Allister J, McKinstry B, McLauglin K, Brennan GP, Forbes AB, Fairweather I (2007) *Fasciola hepatica*: ultrastructural effects of a combination of triclabendazole and clorsulon against mature fluke. Parasitol Res 100:1091–1104

Merino G, Molina AJ, García JL, Pulido MM, Prieto JG, Álvarez AI (2003a) Intestinal elimination of albendazole sulfoxide: pharmacokinetic effects of inhibitors. Int J Pharmaceut 263:123–132

Merino G, Molina J, García L, Pulido MM, Prieto G, Alvarez AI (2003b) Effect of clotrimazole on microsomal metabolism and pharmacokinetics of albendazole. J Pharm Pharmacol 55:757–764

Mottier L, Virkel G, Solana H, Alvarez L, Salles J, Lanusse CE (2004) Triclabendazole biotransformation and comparative diffusion of the parent drug and its oxidized metabolites into *Fasciola hepatica*. Xenobiotica 34:1043–1047

Mottier L, Alvarez L, Ceballos L, Lanusse CE (2006a) Drug transport mechanisms in helminth parasites: passive diffusion of benzimidazole anthelmintics. Exp Parasitol 113:49–57

Mottier L, Alvarez L, Fairweather I, Lanusse CE (2006b) Resistance-induced changes in triclabendazole transport in *Fasciola hepatica*: ivermectin reversal effect. J Parasitol 92:1355–1360

Newton DJ, Wang RW, Lu AYH (1995) Cytochrome P450 inhibitors: evaluation of specificities in the *in vitro* metabolism of therapeutic agents by human liver microsomes. Drug Metab Dispos 23:154–158

Prichard RK, Hennessy DR, Steel JW, Lacey E (1985) Metabolite concentrations in plasma following treatment of cattle with five anthelmintics. Res Vet Sci 39:173–178

Ridtitid W, Wongnawa M, Mahatthanatrakul W, Raungsri N, Sunbhanich M (2005) Ketoconazole increases plasma concentrations of antimalarial mefloquine in healthy human volunteers. J Clin Pharm Ther 30:285–290

Ridtitid W, Ratsamemonthon K, Mahatthanatrakul W, Wongnawa M (2007) Pharmacokinetic interaction between ketoconazole and praziquantel in healthy volunteers. J Clin Pharm Ther 32:585–593

Robinson MW, Trudgett A, Hoey EM, Fairweather I (2002) Triclabendazole-resistant *Fasciola hepatica*: β-tubulin and response to *in vitro* treatment with triclabendazole. Parasitology 124:325–338

Robinson MW, Lawson J, Trudgett A, Hoey EM, Fairweather I (2004) The comparative metabolism of triclabendazole sulphoxide by triclabendazole-susceptible and triclabendazole-resistant *Fasciola hepatica*. Parasitol Res 92:205–210

Saeed HM, Mostafa MH, O'Connor PJ, Rafferty JA, Doenhoff MJ (2002) Evidence for the presence of active cytochrome P450 systems in *Schistosoma mansoni* and *Schistosoma haematobium* adult worms. FEBS Lett 519:205–209

Sánchez S, Small J, Jones DG, McKellar QA (2002) Plasma achiral and chiral pharmacokinetic behavior of intravenous oxfendazole co-administered with piperonyl butoxide in sheep. J Vet Pharmacol Ther 25:7–13

Sánchez-Bruni SFS, Fusé LA, Moreno L, Saumell CA, Álvarez LI, Fiel C, McKellar QA, Lanusse CE (2005) Changes to oxfendazole chiral kinetics and anthelmintic efficacy induced by piperonyl butoxide in horses. Equine Vet J 37:257–262

Solana HD, Rodriguez JA, Lanusse CE (2001) Comparative metabolism of albendazole and albendazole sulphoxide by different helminth parasites. Parasitol Res 87:275–280

Solana H, Scarcella S, Virkel G, Ceriani C, Rodríguez J, Lanusse CE (2009) Albendazole enantiomeric metabolism and binding to cytosolic proteins in the liver fluke *Fasciola hepatica*. Vet Res Commun 33:163–173

Toner E, McConvery F, Brennan GP, Meaney M, Fairweather I (2009) A scanning electron microscope study on the route of entry of triclabendazole into the liver fluke, *Fasciola hepatica*. Parasitology 136:523–535

Toner E, McConvery F, Brennan GP, Meaney M, Fairweather I (2010) A transmission electron microscope study on the route of entry of triclabendazole into the liver fluke, *Fasciola hepatica*. Parasitology (in press)

Virkel G, Lifschitz A, Sallovitz J, Pis A, Lanusse C (2006) Assessment of the main metabolism pathways for the flukicidal compound triclabendazole in sheep. J Vet Pharmacol Ther 29:213–223

Virkel G, Lifschitz A, Sallovitz J, Ballent M, Scarcella S, Lanusse C (2009) Inhibition of cytochrome P450 activity enhances the systemic availability of triclabendazole metabolites in sheep. J Vet Pharmacol Ther 32:79–86

Walker SM, McKinstry B, Boray JC, Brennan GP, Trudgett A, Hoey EM, Fletcher H, Fairweather I (2004) Response of two isolates of *Fasciola hepatica* to treatment with triclabendazole in vivo and in vitro. Parasitol Res 94:427–438

Wen H, New RRC, Muhmut M, Wang JH, Wang YH, Zhang JH, Shao YM, Craig PS (1996) Pharmacology and efficacy of liposome-entrapped albendazole in experimental secondary alveolar echinococcosis and effect of co-administration with cimetidine. Parasitology 113:111–121

Wisedpanichkij R, Chaijaroenkul W, Sangsuwan P, Tantisawat J, Boonprasert K, Na-Bangchang K (2009) *In vitro* antimalarial interactions between mefloquine and cytochrome P450 inhibitors. Acta Trop 112:12–15

Zhang W, Ramamoorthy Y, Kilicarslan T, Nolte H, Tyndale RF, Sellers EM (2002) Inhibition of cytochromes P450 by antifungal imidazole derivatives. Drug Metab Dispos 30:314–318